Submitted: 10 September, 2023 Accepted: 18 October, 2023 Published: 03 May, 2024 DOI:10.22514/jocpd.2024.059

ORIGINAL RESEARCH

Journal of Clinical Pediatric Dentistry

Image segmentation of impacted mesiodens using deep learning

Hyuntae Kim[1], Ji-Soo Song[2], Teo Jeon Shin[2], Young-Jae Kim[2], Jung-Wook Kim[2], Ki-Taeg Jang[2], Hong-Keun Hyun[2,*]

[1]Department of Pediatric Dentistry, Seoul National University Dental Hospital, 03080 Seoul, Republic of Korea
[2]Department of Pediatric Dentistry, Dental Research Institute, School of Dentistry, Seoul National University, 03080 Seoul, Republic of Korea

***Correspondence**
hege1@snu.ac.kr
(Hong-Keun Hyun)

Abstract

This study aimed to evaluate the performance of deep learning algorithms for the classification and segmentation of impacted mesiodens in pediatric panoramic radiographs. A total of 850 panoramic radiographs of pediatric patients (aged 3–9 years) was included in this study. The U-Net semantic segmentation algorithm was applied for the detection and segmentation of mesiodens in the upper anterior region. For enhancement of the algorithm, pre-trained ResNet models were applied to the encoding path. The segmentation performance of the algorithm was tested using the Jaccard index and Dice coefficient. The diagnostic accuracy, precision, recall, F1-score and time to diagnosis of the algorithms were compared with those of human expert groups using the test dataset. Cohen's kappa statistics were compared between the model and human groups. The segmentation model exhibited a high Jaccard index and Dice coefficient (>90%). In mesiodens diagnosis, the trained model achieved 91–92% accuracy and a 94–95% F1-score, which were comparable with human expert group results (96%). The diagnostic duration of the deep learning model was 7.5 seconds, which was significantly faster in mesiodens detection compared to human groups. The agreement between the deep learning model and human experts is moderate (Cohen's kappa = 0.767). The proposed deep learning algorithm showed good segmentation performance and approached the performance of human experts in the diagnosis of mesiodens, with a significantly faster diagnosis time.

Keywords

Artificial intelligence; Mesiodens; Deep learning; U-Net; Semantic segmentation; Panoramic radiography

1. Introduction

The panoramic radiograph is an imaging technique used in dentistry primarily to diagnose oral and maxillofacial diseases. Panoramic radiographs have the advantage of displaying multiple anatomical structures in a single image, but lesions are difficult to interpret due to their low image resolution and the presence of overlapping structures in mixed dentition [1, 2]. Panoramic radiographs are routinely used to evaluate the eruption and development of teeth in a clinical setting, and supernumerary teeth in the anterior region (mesiodens) are one of the most commonly identified anomalies [3].

Supernumerary teeth result from the proliferation of dental lamina and are more prevalent in the anterior regions than in the posterior [4]. The etiology of supernumerary teeth has not been conclusively determined [5], but genetic and environmental factors are believed to play a role [6]. The incidence of mesiodens is estimated to be 0.15–3.18% [7]. Studies on the Korean population indicate a prevalence range of 2.0–3.4%, which is higher than reported in the United States and Europe [8, 9]. Impacted mesiodens may cause a variety of dental issues, including eruption disturbance of permanent incisors, diastema, crowding and dentigerous cysts. Therefore, timely surgical removal of impacted mesiodens is essential for harmonious occlusion in pediatric patients [10].

In recent years, numerous research investigations on artificial intelligence have been conducted in various fields of medicine [11–15]. In the field of dentistry, analysis of the efficacy of deep learning models as a diagnostic aid has been a primary focus [16–18]. As anatomical structures of the oral and maxillofacial regions are visible in panoramic radiographs, much time and effort are necessary for an accurate diagnosis. There is a need for a diagnostic instrument for lesions on panoramic radiographs to increase the efficiency and accuracy of diagnosis.

Semantic segmentation, a deep learning algorithm, can be used to predict the class of each pixel of a panoramic radiograph image and to locate the boundary of a structure [19, 20]. The purpose of our study was to compare the diagnostic performance between a trained model and human expert groups by performing semantic segmentation to find impacted mesiodens in panoramic radiographs of pediatric

patients. Therefore, the results of the better-performing group may be used to set goals for groups of dental school students.

2. Materials and methods

2.1 Subjects

From January 2015 to December 2020, 850 panoramic radiographs were performed on children (age range, 3–9 years) who visited the Department of Pediatric Dentistry at the Seoul National University Dental Hospital for the diagnosis of mesiodens. These 850 images were included in the study. All panoramic radiographs were acquired using OP-100 (Instrumentarium Dental, Tuusla, Finland) and Rayscan Alpha-P (Ray Co., Gyeonggi, Korea). The exclusion criteria were developmental anomalies such as cleft lip or palate and orthodontic appliances attached to the maxilla. The 850 panoramic radiographs were composed of 830 radiographs with impacted mesiodens and 20 radiographs without mesiodens. Of these, 750 radiographs were used to train the deep learning model, while 100 radiographs were used as test data and composed of 80 radiographs with mesiodens and 20 radiographs without mesiodens. The average age of the subjects was 6.0 ± 2.0 years; 59.9% of the patients were male and 40.1% were female. Among the 830 panoramic radiographs with mesiodens, 513 (61.8%) were inverted, 97 (11.7%) were horizontal, and 220 (26.5%) were in the normal direction. There were 637 (76.7%) cases with one impacted mesiodens, 192 (23.2%) cases with two, and just one (0.1%) case with three mesiodens (Table 1).

2.2 Preprocessing of data

All panoramic radiographs were acquired in JPEG format (2560 × 1500 pixels) from the INFINITT G3 PACS system (INFINITT Healthcare Co. Ltd., Seoul, Korea). A region of interest (ROI) was established at the center of the anterior maxilla to facilitate efficient learning with limited computer resources. The ROI was the area bounded by the distal plane of the permanent lateral incisors on the left and right sides, the base of the nasal cavity, and the incisal plane of the erupted maxillary anterior teeth. An experienced dentist cropped the ROI from the acquired panoramic image files using Adobe Photoshop 23.0 (Adobe Systems Inc., San Jose, CA, USA).

Two pediatric dentists with three and four years of experience, respectively, annotated the position and boundaries of mesiodens on panoramic radiographs, and the presence of mesiodens was confirmed with cone beam computed tomography (CBCT). For annotation, the open-source software Computer Vision Annotation Tool (CVAT, Intel Corporation, Santa Clara, CA, USA) was used. The interobserver reliability coefficient between the two observers was 0.964, while the intraobserver agreement for observer 1 and observer 2 was 0.973 and 0.957, respectively. The annotated data were exported in binary mask format (Fig. 1).

2.3 Development and evaluation of the model

The mesiodens segmentation model was developed utilizing the U-Net [21] algorithm with modifications to the encoder using ResNet18, ResNet34 and ResNet50. The U-Net is a type of semantic segmentation algorithm developed primarily for segmenting medical images and known for yielding exceptional segmentation performance [22].

The annotated binary information and cropped panoramic images were used for training the deep learning models. All models were trained up to 250 times using our dataset with the batch size of 16 and learning rate of 0.001. The segmentation performance was evaluated based on the Jaccard

TABLE 1. Characteristics of the subjects in this study.

Characteristics	Patients with Mesiodens (n = 830)	Patients without Mesiodens (n = 20)	Total (n = 850)
Mean Age (SD)	6.1 (2.1)	6.6 (2.0)	6.0 (2.0)
Gender			
Female	333 (40.1%)	8 (40.0%)	341 (40.1%)
Male	497 (59.9%)	12 (60.0%)	509 (59.9%)
Dentition			
Primary	180 (21.7%)	5 (25.0%)	185 (21.8%)
Mixed	650 (78.3%)	15 (75.0%)	665 (78.2%)
Number of mesiodens			
One	637 (76.8%)		
Two	192 (23.1%)		
Three	1 (0.1%)		
Eruption direction			
Normal	220 (26.5%)		
Inverted	513 (61.8%)		
Horizontal	97 (11.7%)		

SD: Standard deviation.

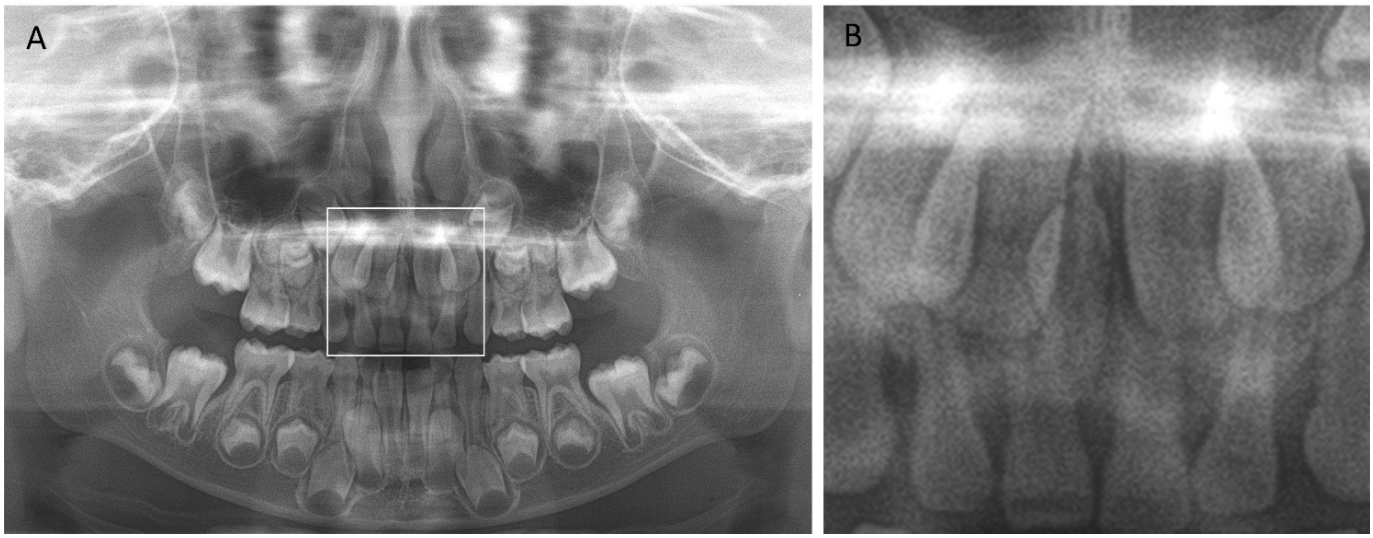

FIGURE 1. Region of interest (ROI). (A) Panoramic radiograph with an ROI bounding box. (B) Cropped image from a panoramic radiograph.

index (1) [23] and Dice coefficient (2) [24]. Training and validation processes were implemented in the Fastai library framework with modifications based on the PyTorch deep learning framework [25]. All processes were implemented in a Google Collaboratory (Google LLC, Mountain View, CA, USA) cloud computing environment using an NVIDIA Tesla K80s graphical processing unit (NVIDIA, Santa Clara, CA, USA) with 12 GB of video memory and 4992 Compute Unified Device Architecture (CUDA) cores.

$$Jaccard\ index = \frac{|MS \cap GT|}{|MS \cup GT|} \quad (1)$$

$$Dice\ coefficient = \frac{2\,|MS \cap GT|}{|MS| + |GT|} \quad (2)$$

MS: Machine segmentation; GT: Ground truth.

2.4 Comparison with expert groups

To evaluate the efficacy of the deep learning algorithm in a clinical environment, a comparison was conducted with human expert groups. According to their expertise in diagnosing mesiodens, the human experts were divided into three groups: pediatric dentists (PS), general dental practitioners (GP), and dental school students (ST). The PS group consisted of five pediatric dental specialists with three to five years of experience. The GP group was composed of five general dentists who had three years of clinical experience, while the ST group consisted of five dental school students with limited clinical experience. The mesiodens were segmented using 100 test datasets, and the results were compared to the ground truth. The Jaccard index value was evaluated using a 50% cut-off threshold, indicating that the diagnosis is accurate if more than 50% of the model segmentation overlaps with the ground truth. To determine the average time required to diagnose mesiodens in a panoramic radiograph, each participant was provided enough time to become familiar with the annotation tool, and then the time required to diagnose 10 additional radiographs was measured. The accuracy (3), precision (4), recall (5), F1-score (6), and time for diagnosis were used to evaluate the performance of the deep learning models and expert groups.

$$Accuracy = \frac{TP + TN}{TP + TN + FP + FN} \quad (3)$$

$$Precision = \frac{TP}{TP + FP} \quad (4)$$

$$Recall = \frac{TP}{TP + FN} \quad (5)$$

$$F1 - score = 2 \times \frac{Recall \times Precision}{Recall + Precision} \quad (6)$$

TP: true positive; FP: false positive; FN: false negative; and TN: true negative.

2.5 Statistical analysis

Measurements were presented as the median and interquartile range, and the Kruskal-Wallis test was employed to compare the performance of deep learning models to that of expert groups. Interobserver agreement with respect to the presence/absence of mesiodens in the test dataset was calculated using Cohen's kappa. The kappa values were classified as follows: 0, poor; 0.00–0.20, weak; 0.21–0.40, fair; 0.41–0.60, moderate; 0.61–0.80, substantial; and 0.81–1.00, almost perfect agreement [26]. For statistical analysis, SPSS 26.0 (SPSS Inc., IBM, Chicago, IL, USA) was used, and the significance level (α) was set to 0.05.

3. Results

3.1 Performance evaluation of the deep learning segmentation model

Table 2 demonstrates the diagnostic performance based on the Jaccard index and Dice coefficient with various encoders. The performance of the model segmentation improved as ResNet layers were added.

TABLE 2. Performance measurements of the Jaccard index and Dice coefficient for different pre-trained deep learning network models.

	Jaccard index	Dice coefficient
U-Net	0.904	0.913
ResNet-18	0.912	0.931
ResNet-34	0.914	0.934
ResNet-50	0.924	0.938

3.2 Comparison of the diagnostic capabilities of a deep learning model with human expert groups

According to the type of encoders used, deep learning models were categorized as U-Net, ResNet18, ResNet34 and ResNet50, while expert groups were classified as pediatric dentists (PS), general dentists (GP) and dental school students (ST). Table 3 displays the diagnostic ability of each group using a 50% Jaccard index as the diagnostic criteria cutoff. The accuracy, precision, recall and F1-score were statistically different among the groups. The F1-score of the PS group was 0.99, demonstrating the best diagnostic ability, followed by that of GP with 0.96. With the deep learning algorithm, the F1-score was 0.95, comparable to those of the GP groups. The diagnostic accuracy of ST was lower than that of the other groups. The deep learning algorithm was faster in diagnosis at 6–8 seconds compared to all the expert groups. The deep learning model used an average diagnosis time of 0.075 seconds per image, which was faster than the expert groups ($p < 0.05$, Table 3 and Fig. 2). Results showed that the deep learning algorithms were superior in diagnostic time and exhibited comparable diagnostic performance to general dentists. Interobserver agreements were measured between the best-performing individuals from each group and the best artificial intelligence (AI) model (ResNet-50). There was almost perfect agreement (kappa value = 0.852) between the best pediatric dentist (BPS) and the best general dental practitioner (BGP). However, the agreement between BPS and the best AI model (BAI) was moderate (kappa value = 0.767). Finally, there was fair agreement (kappa value = 0.571) between BPS and the best dental school student (BST) (Table 4).

4. Discussion

Panoramic radiographs are the basic method for detecting mesiodens. They can capture a complete image of the teeth and jawbones in a single scan without the discomfort inherent to inserting a film in the oral cavity. Therefore, this is an effective method for obtaining radiographic images with minimal cooperation from pediatric patients. However, using panoramic radiography alone to diagnose mesiodens is questionable [27]. Consequently, periapical radiographs from various angles, occlusal radiographs, and CBCTs are additionally performed in clinical settings [10, 28]. CBCTs are one of the most accurate diagnostic modalities available. However, in clinical settings where CBCTs are not available, the use of panoramic radiographs in addition to periapical and occlusal radiographs would still be considered a beneficial diagnostic tool for the dentist to learn to identify impacted mesiodens.

Studies utilizing artificial intelligence algorithms to identify mesiodens on panoramic radiographs have been conducted, and the algorithm models successfully identified mesiodens [29–31]. Ahn *et al.* [29] reported significant time savings with deep learning models in detecting mesiodens, with 1.5 ± 1.4 seconds for diagnosis compared to 811.8 ± 426.1 seconds for general practitioners. In semantic segmentation, various artificial models have been applied to automated teeth segmentation [32, 33], dental caries detection [34, 35], detection of third molars and mandibular nerves [36], dental restorations [37], and ectopic eruption of teeth [38]. They demonstrated effective performance with significantly reduced diagnostic time. However, there is a lack of research evaluating the performance of the segmentation models of supernumerary teeth in pediatric panoramic radiographs.

TABLE 3. Diagnostic performance of the deep learning models and human expert groups.

	Accuracy	Precision	Recall	F1-score	Time for diagnosis(s)
PS	0.99 (0.98–1.00)	0.99 (0.97–1.00)	1.00 (1.00–1.00)	0.99 (0.98–1.00)	540 (530–547)
GP	0.93 (0.92–0.95)	0.97 (0.96–0.98)	0.95 (0.91–0.96)	0.96 (0.95–0.97)	643 (620–645)
ST	0.83 (0.81–0.85)	0.89 (0.88–0.89)	0.88 (0.87–0.90)	0.89 (0.88–0.90)	834 (810–840)
U-Net	0.91	0.95	0.92	0.94	7 (6–8)
ResNet-18	0.92	0.95	0.93	0.95	
ResNet-34	0.92	0.96	0.95	0.95	
ResNet-50	0.92	0.97	0.95	0.95	

Values are presented as median (inter-quartile range) or number.
PS: Pediatric dentists, GP: General dental practitioners, ST: Dental school students.

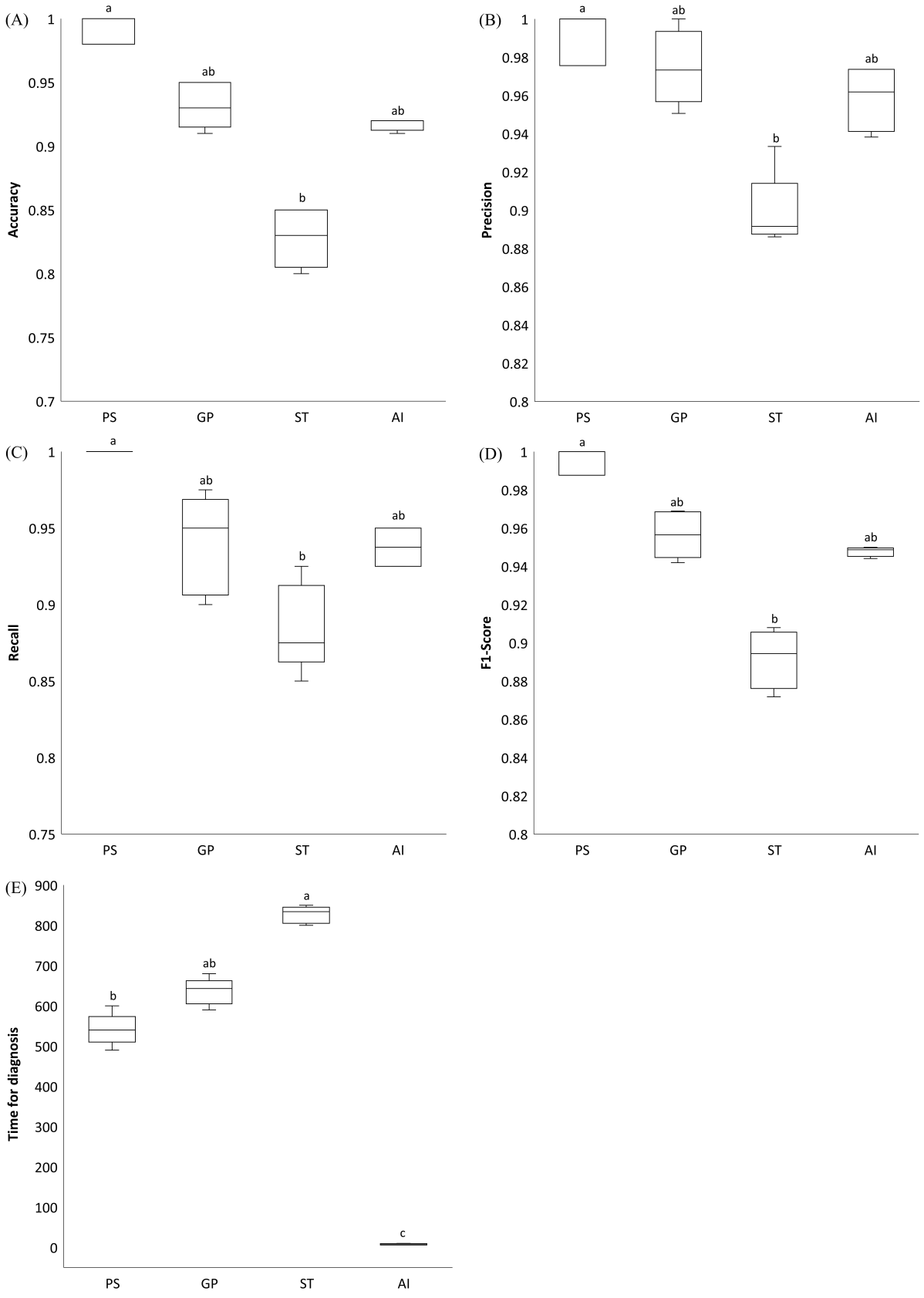

FIGURE 2. Boxplot of the diagnostic performance among the AI and human groups. The Kruskal-Wallis test and Bonferroni-corrected Mann Whitney U test as *post hoc* tests were performed to analyze the statistical significance of (A) accuracy, (B) precision, (C) recall, (D) F1-score, and (E) time for diagnosis. The same superscript indicates no significant difference between the groups. PS: Pediatric dentists, GP: General dental practitioners, ST: Dental school students, AI: Deep learning models.

TABLE 4. Interobserver agreement data.

	BAI versus BPS	BGP versus BPS	BST versus BPS
Kappa	0.767	0.852	0.571
p-value	<0.0001	<0.0001	<0.0001

BPS: the best pediatric dentist; BGP: the best general dental practitioner; BST: the best dental school student; BAI: the best AI model.
Interobserver agreement was measured using Cohen's unweighted kappa.

In this study, the deep learning model utilizing the U-Net algorithm for segmentation had a Jaccard index greater than 90% and a Dice coefficient greater than 91% with all the algorithm models demonstrating high segmentation performance. The deep learning model was similarly effective for the group of general dentists. The F1-scores obtained from the deep learning model were similar to those of general dentists. However, the interquartile range values were comparatively lower. The effectiveness of the algorithm, which was trained on a small dataset, is insufficient to replace pediatric dentists. However, with a diagnostic time of 7 seconds on average for each of the 100 test radiographs, the algorithm demonstrated remarkable efficiency. Based on our limited results, the current deep learning model's ability to diagnose mesiodens may be considered to perform at the level of a general dentist. In the future, we believe that the amount of data included in training should be increased to achieve diagnostic performance at the level of pediatric dentists. If it is improved and developed into a highly trained model, it is expected to reduce the time and effort spent on diagnosis by clinicians in clinical practice, and the diagnosis of this deep learning model may be used as a second opinion to reconfirm their diagnosis and improve the completeness of their diagnosis.

This study has several limitations. First, only the supernumerary teeth that were impacted in the anterior part of the maxilla were included. Due to the limited computer resources required for learning and optimizing the learning process, a decision was made to establish a small ROI. Therefore, the trained models exhibited limited ability to diagnose outside the designated ROI. In future studies, a wider area of interest and a larger number of cases in the learning model should be included to improve the diagnostic ability. Second, in setting the ground truth, as two pediatric dentists directly marked the location of the supernumerary teeth, subjective views and observational errors may be included. Last, the current study was carried out with data from a single hospital, limiting the universal applicability of the results. With larger datasets from multi-center institutions and a wider ROI that includes entire panoramic radiographs, the deep learning model can be more useful in the future for diagnosis based on radiographs. The results may be applied to the diagnosis of other pathologies in pediatric patients such as ankylosed teeth, impacted canines, ectopic eruption of permanent teeth, and traumatized teeth.

5. Conclusions

In this study, a deep learning model was developed to detect and segment impacted mesiodens in panoramic radiographs of pediatric patients. Using a semantic segmentation technique based on the U-Net, the model successfully segmented impacted mesiodens with accuracy greater than 90%. The mesiodens detection accuracy was greater than 91% on the test dataset. Therefore, the diagnostic performance of the deep learning model is comparable to that of a general dentist, with the advantage of faster diagnostic time.

AVAILABILITY OF DATA AND MATERIALS

The data presented in this study are available on reasonable request from the corresponding author.

AUTHOR CONTRIBUTIONS

HK, YJK, JWK and HKH—designed the research study. HK, JSS and HKH—performed the research. TJS and KTJ—provided help and advice on the technical and statistical analysis. HK, HKH and YJK—analyzed the data. HK, JSS and JWK—wrote the original manuscript. HKH, TJS, YJK and KTJ—reviewed and edited the original manuscript. All authors contributed to editorial changes in the manuscript. All authors read and approved the final manuscript.

ETHICS APPROVAL AND CONSENT TO PARTICIPATE

This study was approved by the Institutional Review Board of the Seoul National University Dental Hospital (IRB No: ERI21038). The Institutional Review Board of the Seoul National University Dental Hospital waived the requirement of informed consent for the use of retrospective data, so written or verbal informed consent was not obtained from any participants.

ACKNOWLEDGMENT

Not applicable.

FUNDING

This research received no external funding.

CONFLICT OF INTEREST

The authors have no potential conflicts of interest to disclose. Hong-Keun Hyun is serving as the Editorial Board member and Guest Editor of this journal. We declare that Hong-Keun Hyun had no involvement in the peer review of this article and has no access to information regarding its peer review. Full responsibility for the editorial process for this article was delegated to ALG.

REFERENCES

[1] Perschbacher S. Interpretation of panoramic radiographs. Australian Dental Journal. 2012; 57: 40–45.

[2] Leite AF, Gerven AV, Willems H, Beznik T, Lahoud P, Gaêta-Araujo H, *et al*. Artificial intelligence-driven novel tool for tooth detection and segmentation on panoramic radiographs. Clinical Oral Investigations. 2021; 25: 2257–2267.

[3] Asaumi J, Hisatomi M, Yanagi Y, Unetsubo T, Maki Y, Matsuzaki H, *et al*. Evaluation of panoramic radiographs taken at the initial visit at a department of paediatric dentistry. Dentomaxillofacial Radiology. 2008; 37: 340–343.

[4] Omer RS, Anthonappa RP, King NM. Determination of the optimum time for surgical removal of unerupted anterior supernumerary teeth. Pediatric Dentistry. 2010; 32: 14–20.

[5] Rajab LD, Hamdan MAM. Supernumerary teeth: review of the literature and a survey of 152 cases. International Journal of Paediatric Dentistry. 2002; 12: 244–254.

[6] Ata-Ali F, Ata-Ali J, Penarrocha-Oltra D, Penarrocha-Diago M. Prevalence, etiology, diagnosis, treatment and complications of supernumerary teeth. Journal of Clinical and Experimental Dentistry. 2014; 6: e414–e418.

[7] Asaumi J, Shibata Y, Yanagi Y, Hisatomi M, Matsuzaki H, Konouchi H, *et al*. Radiographic examination of mesiodens and their associated complications. Dentomaxillofacial Radiology. 2004; 33: 125–127.

[8] Kim SG, Lee SH. Mesiodens: a clinical and radiographic study. Journal of Dentistry for Children. 2003; 70: 58–60.

[9] Mukhopadhyay S. Mesiodens: a clinical and radiographic study in children. Journal of Indian Society of Pedodontics and Preventive Dentistry. 2011; 29: 34–38.

[10] Ayers E, Kennedy D, Wiebe C. Clinical recommendations for management of mesiodens and unerupted permanent maxillary central incisors. European Archives of Paediatric Dentistry. 2014; 15: 421–428.

[11] Shen D, Wu G, Suk H. Deep learning in medical image analysis. Annual Review of Biomedical Engineering. 2017; 19: 221–248.

[12] Esteva A, Chou K, Yeung S, Naik N, Madani A, Mottaghi A, *et al*. Deep learning-enabled medical computer vision. npj Digital Medicine. 2021; 4: 5.

[13] Wang J, Zhu H, Wang S, Zhang Y. A review of deep learning on medical image analysis. Mobile Networks and Applications. 2021; 26: 351–380.

[14] Bayraktar Y, Ayan E. Diagnosis of interproximal caries lesions with deep convolutional neural network in digital bitewing radiographs. Clinical Oral Investigations. 2022; 26: 623–632.

[15] Cejudo JE, Chaurasia A, Feldberg B, Krois J, Schwendicke F. Classification of dental radiographs using deep learning. Journal of Clinical Medicine. 2021; 10: 1496.

[16] Cantu AG, Gehrung S, Krois J, Chaurasia A, Rossi JG, Gaudin R, *et al*. Detecting caries lesions of different radiographic extension on bitewings using deep learning. Journal of Dentistry. 2020; 100: 103425.

[17] Lee JH, Jeong SN. Efficacy of deep convolutional neural network algorithm for the identification and classification of dental implant systems, using panoramic and periapical radiographs: a pilot study. Medicine. 2020; 99: e20787.

[18] Lee S, Oh SI, Jo J, Kang S, Shin Y, Park JW. Deep learning for early dental caries detection in bitewing radiographs. Scientific Reports. 2021; 11: 16807.

[19] Wang P, Chen P, Yuan Y, Liu D, Huang Z, Hou X, *et al*. Understanding convolution for semantic segmentation. 2018 IEEE Winter Conference on Applications of Computer Vision. IEEE: Lake Tahoe. 2018.

[20] Jiang F, Grigorev A, Rho S, Tian Z, Fu Y, Jifara W, *et al*. Medical image semantic segmentation based on deep learning. Neural Computing and Applications. 2018; 29: 1257–1265.

[21] Ronneberger O, Fischer P, Brox T. U-Net: convolutional networks for biomedical image segmentation. Lecture Notes in Computer Science. 2015; 1: 234–241.

[22] Du G, Cao X, Liang J, Chen X, Zhan Y. Medical image segmentation based on U-Net: a review. Journal of Imaging Science & Technology. 2020; 64: 1–12.

[23] Jaccard P. The distribution of the flora in the alpine zone. New Phytologist. 1912; 11: 37–50.

[24] Sorenson T. A method of establishing groups of equal amplitude in plant sociology based on similarity of species content, and its application to analysis of vegetation on Danish commons. Kongelige Danske Videnskabernes Selskab, Biologiske Skrifter. 1948; 5: 1–34.

[25] Howard J, Gugger S. Fastai: a layered API for deep learning. Information. 2020; 11: 108.

[26] Landis JR, Koch GG. The measurement of observer agreement for categorical data. Biometrics. 1977; 33: 159–174.

[27] Matteson SR, Lupton CR, Morrison WS. Effect of panoramic focal trough topography on radiographic imaging of supernumerary teeth in the anterior region. Journal of Oral and Maxillofacial Surgery. 1982; 40: 318–319.

[28] Itaya S, Oka K, Kagawa T, Oosaka Y, Ishii K, Kato Y, *et al*. Diagnosis and management of mesiodens based on the investigation of its position using cone-beam computed tomography. Pediatric Dental Journal. 2016; 26: 60–66.

[29] Ahn Y, Hwang JJ, Jung YH, Jeong T, Shin J. Automated mesiodens classification system using deep learning on panoramic radiographs of children. Diagnostics. 2021; 11: 1477.

[30] Kim J, Hwang JJ, Jeong T, Cho B, Shin J. Deep learning-based identification of mesiodens using automatic maxillary anterior region estimation in panoramic radiography of children. Dentomaxillofacial Radiology. 2022; 51: 20210528.

[31] Ha EG, Jeon KJ, Kim YH, Kim JY, Han SS. Automatic detection of mesiodens on panoramic radiographs using artificial intelligence. Scientific Reports. 2021; 11: 23061.

[32] Arora S, Tripathy SK, Gupta R, Srivastava R. Exploiting multimodal CNN architecture for automated teeth segmentation on dental panoramic X-ray images. Proceedings of the Institution of Mechanical Engineers, Part H: Journal of Engineering in Medicine. 2023; 237: 395–405.

[33] Lee J, Han S, Kim YH, Lee C, Kim I. Application of a fully deep convolutional neural network to the automation of tooth segmentation on panoramic radiographs. Oral Surgery, Oral Medicine, Oral Pathology and Oral Radiology. 2020; 129: 635–642.

[34] Bayrakdar IS, Orhan K, Akarsu S, Çelik Ö, Atasoy S, Pekince A, *et al*. Deep-learning approach for caries detection and segmentation on dental bitewing radiographs. Oral Radiology. 2022; 38: 468–479.

[35] Ying S, Wang B, Zhu H, Liu W, Huang F. Caries segmentation on tooth X-ray images with a deep network. Journal of Dentistry. 2022; 119: 104076.

[36] Vinayahalingam S, Xi T, Bergé S, Maal T, de Jong G. Automated detection of third molars and mandibular nerve by deep learning. Scientific Reports. 2019; 9: 9007.

[37] Oztekin F, Katar O, Sadak F, Aydogan M, Yildirim TT, Plawiak P, *et al*. Automatic semantic segmentation for dental restorations in panoramic radiography images using U-Net model. International Journal of Imaging Systems and Technology. 2022; 32: 1990–2001.

[38] Zhu H, Yu H, Zhang F, Cao Z, Wu F, Zhu F. Automatic segmentation and detection of ectopic eruption of first permanent molars on panoramic radiographs based on nnU-Net. International Journal of Paediatric Dentistry. 2022; 32: 785–792.

How to cite this article: Hyuntae Kim, Ji-Soo Song, Teo Jeon Shin, Young-Jae Kim, Jung-Wook Kim, Ki-Taeg Jang, *et al*. Image segmentation of impacted mesiodens using deep learning. Journal of Clinical Pediatric Dentistry. 2024; 48(3): 52-58. doi: 10.22514/jocpd.2024.059.